Quaternary Research 81 (2014) 513–519

Contents lists available at ScienceDirect

Quaternary Research

journal homepage: www.elsevier.com/locate/yqres

# Early-summer temperature variations over the past 563 yr inferred from tree rings in the Shaluli Mountains, southeastern Tibet Plateau

Yang Deng [a], Xiaohua Gou [a,*], Linlin Gao [a], Tao Yang [a], Meixue Yang [b]

[a] MOE Key Laboratory of Western China's Environmental Systems, Collaborative Innovation Centre for Arid Environments and Climate Change, Lanzhou University, Lanzhou 73000, China
[b] State Key Laboratory of Cryospheric Sciences, Cold and Arid Regions Environmental and Engineering Research Institute, Chinese Academy of Sciences, Lanzhou 730000, China

ARTICLE INFO

*Article history:*
Received 11 February 2013
Available online 30 August 2013

*Keywords:*
Tree rings
Temperature reconstruction
Climate variability
Southeastern Tibet Plateau

ABSTRACT

We developed a tree-ring chronology (AD 1446–2008) based on 75 cores from 37 *Abies squamata* Mast. trees from the Shaluli Mountains, southeastern Tibet Plateau, China, using signal-free methods, which are ideally suited to remove or reduce the distortion introduced during traditional standardization. This chronology correlates best with regional temperatures in June–July, which allowed us to develop a June–July temperature reconstruction that explained 51.2% of the variance in the instrumental record. The reconstruction showed seven cold periods and five warm periods. Cold periods were identified from AD 1472 to 1524, 1599 to 1653, 1661 to 1715, 1732 to 1828, 1837 to 1847, 1865 to 1876 and 1907 to 1926. Warm intervals occurred from AD 1446 to 1471, 1525 to 1598, 1716 to 1731, 1848 to 1864, 1877 to 1906 and 1927 to present. The reconstruction agrees well with nearby tree-ring-based temperature reconstructions. Spatial correlation analyses suggest that our reconstructions provide information on June–July temperature variability for the southeastern Tibetan Plateau and its vicinity. Spectral analyses revealed significant peaks at 2–6, 10.7, 51.2, 102.2 and 204.8 yr. The temperature variability in this area may be affected by ENSO, the Pacific Decadal Oscillation and solar activity.



## Introduction

Global warming is a public concern because it has a significant impact on ecosystems and on the stability of the social economy. However, the observed temperature changes vary over the northern hemisphere; therefore, understanding regional temperature variations is vitally important (IPCC, 2007). On the southeastern Tibet Plateau, precise instrumental measurements of temperature began only in the early 1950s; this short temperature record is inadequate for characterizing regional variability. Therefore, obtaining temperature variation information from proxy data is essential to improving our understanding of regional temperature variation.

Tree rings provide one of the best known and most used proxies for reconstructing climate variation over the past centuries and millennia (IPCC, 2007). In southeastern Tibet Plateau, several tree-ring-based temperature reconstructions have been conducted. These previous studies used quantities including tree-ring width, $\delta^{13}C$ and the maximum density of the latewood as proxies, to reconstruct climate variables such as wintertime, summertime and extreme (both maximum and minimum) temperatures over periods ranging from approximately 100 to 409 yr (Shao and Fan, 1999; Wu et al., 2005; Song et al., 2007; Duan et al., 2010; Li et al., 2010; Xu et al., 2010; Li et al., 2011; Yu et al., 2012).

However, none of these studies are situated in the northern part of the Shaluli Mountains, southeastern Tibet Plateau, so it is important to conduct tree-ring studies in this area. Moreover, some studies found that significant differences occur between seasons. For example, in the North Atlantic, summers have warmed more rapidly than winters since 1353 (Kamenos, 2010). Moreover, using data from observations and models, Cohen et al. (2012) identified that winter temperature had decreased in the past few decades, despite the current context of unprecedented global warming. Gou et al. (2008) found that the maximum and minimum temperatures on the northeastern Tibetan Plateau have changed asymmetrically in the past 425 yr.

Here, we present a new chronology of tree-ring width for the Shaluli Mountains, southeastern Tibet Plateau over the past 715 yr. The purposes of this study are to explore the climate factors that affect tree growth, reconstruct the temperature reliably to extend the record beyond the instrumental period, identify the spatial validity of the reconstruction and explore possible driving factors through spatial correlation and comparison with other time series.

## Materials and methods

### Study area

Our sampling site at Baiyu (31°08′48″N, 99°47′02″E, 4280–4325 m asl) is situated in the northern part of the Shaluli Mountains, southeastern Tibet Plateau (Fig. 1). The Indian monsoon system is the

* Corresponding author.
*E-mail address:* xhgou@lzu.edu.cn (X. Gou).

0033-5894/$ – see front matter 
http://dx.doi.org/10.1016/j.yqres.2013.08.002

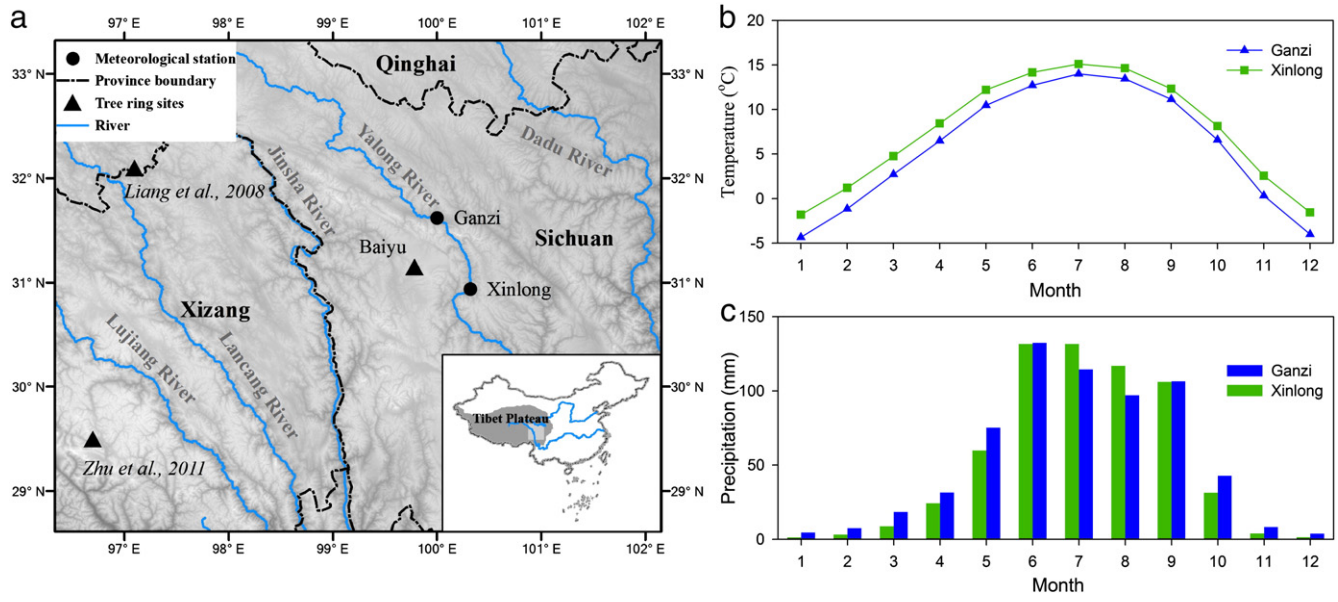


**Figure 1.** Location map of the tree-ring sampling site at Baiyu (31°08′48″N, 99°47′02″E, 4280–4325 m asl), nearby meteorological stations and other tree-ring sites used for comparison (Liang et al., 2008; Zhu et al., 2011) (a); monthly mean temperature (b) and total precipitation (c) records at Ganzi and Xinlong meteorological stations, averaged over 1960–2007.

dominant component of climate in the area; it transports warm, moist air from the Bay of Bengal to the study site in the summer (Domrös and Peng, 1988). Over the 1960–2007 period, mean annual temperature at Ganzi and Xinlong weather stations was 5.7°C and 7.5°C, and mean annual total precipitation was 642 mm and 620 mm, respectively (Fig. 1).

### *Tree-ring data*

To develop a chronology of tree-ring width, tree-ring samples were collected from *Abies squamata* Mast. trees in Baiyu (Fig. 1). One to four cores were obtained from per tree by an increment borer at breast height (1.3 m). A total of 75 radii from 37 trees were collected. In the laboratory, all increment cores were glued to wooden core mounts to dry, then sanded with progressively finer sandpaper, up to 600-grit. Each core was cross-dated to assign each tree ring the exact calendar year of its formation. All tree-ring widths were then measured with 0.001 mm precision with the software Measure J2X. The computer program COFECHA was used to ensure the accuracy of both the cross-dating and measurements (Holmes, 1983).

Age-related trends were removed from the raw data using a cubic smoothing spline with 50% variance reduction at 260 yr, which corresponds to approximately 70% of the mean (375.7 yr) and median (371 yr) segment length. A signal-free version of the computer program ARSTAN (E. R. Cook, personal communication) was used to calculate standard tree-ring chronologies. To reduce the influence of outliers, bi-weight robust means were used to calculate the mean ring-width index (Cook and Kairiukstis, 1990). To reduce the influence of decreasing sample size in the older parts of the chronologies, the chronology variance was stabilized using the "running Rbar" parameter. The inter-series correlation (Rbar) and expressed population signal (EPS) were employed to evaluate the most reliable periods of the chronologies, and satisfactory quality was defined as EPS > 0.85 (Wigley et al., 1984). Both Rbar and EPS were calculated for 51-yr moving windows with 50-yr overlaps. The software provided four chronologies: the standard chronology (StdCrn), the signal-free chronology (SsfCrn), the stabilized standard chronology (StdStb) and the stabilized signal-free chronology (SsfStb). The signal-free chronologies were calculated according to the signal-free standardization approach described by Melvin and Briffa (2008). Signal-free standardization was used because it is ideally suited to remove or reduce the distortion introduced during the traditional standardization. The distortion is most prevalent at the ends of the chronology (Melvin and Briffa, 2008). Only the Rbar-stabilized chronologies were used in following analysis.

### *Climate data*

The closest meteorological stations to the sampling site are Ganzi (31°37′N, 100°00′E, 3394 m asl, Fig. 1) and Xinlong (30°56′N, 100°19′E, 3000 m asl, Fig. 1), both approximately 56 km from the study site. Because our study site is situated between the two stations, we calculated a regional climatological mean for the calibration of our chronology from the climate data from these stations. Climate variables for climate-growth analyses include monthly means of temperature and precipitation for the 48-yr period of 1960–2007. For comparison, the reconstructed North Hemisphere temperature (D'Arrigo et al., 2006) and El Niño-Southern Oscillation (ENSO; Wilson et al., 2010) index, downloaded from http://www.ncdc.noaa.gov/paleo/, were used. The monthly 0.5° × 0.5° gridded temperature dataset from CRU TS 3.1 (Mitchell and Jones, 2005) was also used to assess the spatial representation of the reconstruction.

### *Methods*

To minimize the effect of significantly differing means and variances, the climate data were normalized (zero mean and unit variance) before averaging. These averaged values were then converted back to 'absolute' values using the means and standard deviations of the regional mean climate series, which are calculated by simply averaging the original climate data of the two stations. Pearson correlation coefficients were calculated between the tree-ring chronologies and regional monthly climate variables (precipitation, mean temperature) from prior May to current August. This period contains two growing seasons. In addition, various seasonal means (e.g., June–July) of climate variables and their correlations with tree-ring data were also calculated. The temporal variations of the relationship between the tree-ring chronology and the climate factor were determined using a moving correlation with a 30-yr window and a one-yr step; correlations with a varying

https://doi.org/10.1016/j.yqres.2013.08.002 Published online by Cambridge University Press

start year and a fixed end year, as well as correlations with a fixed start year and a varying end year, were also calculated. The multi-taper method (MTM; Mann and Lees, 1996) was used to identify the dominant periods in the reconstructed temperature series. The MTM with resolution = 2 and tapers = 3 were used. Relevant peaks were identified relative to a red noise background with $p < 0.05$.

## Results and discussion

### *The chronologies*

A standard chronology made with conventional detrending methods and a final (after 33 iterations) signal-free chronology were established over a 715-yr period spanning AD 1294 to 2008. The signal-free chronology exhibits a few subtle differences from the standard chronology, all at low frequencies. The signal-free chronology has higher values in the 16th and 20th centuries and lower values from the 1600 s through the 1870 s. The running Rbar and running EPS were almost identical for the two chronologies. Running EPS values were generally high (Fig. 2), and the threshold of 0.85 was reached at a sample depth of seven cores (three trees) after AD 1446 for both chronologies, with the exception of the period 1491–1498. The following analyses are based only on the reliable portion of the chronology, which runs from 1446 to 2008.

### *Climate–growth relationship*

The correlation of the chronologies with the regional monthly climate data is shown in Figure 3. The StdStb and SsfStb chronologies show generally similar results. The correlations of the SsfStb chronology with climate were generally higher in the tree ring's current growing season, which may be because the traditional standardization process eliminates some of the climate signal. Therefore, the SsfStb chronology was used in the following analysis. A significant ($p < 0.05$) relationship with temperature was found at the current June, the current July, the previous July (although the latter was not significant for the SsfStb chronology) and the previous August, with $p < 0.01$ significance at the current June and previous August. The correlation coefficients for

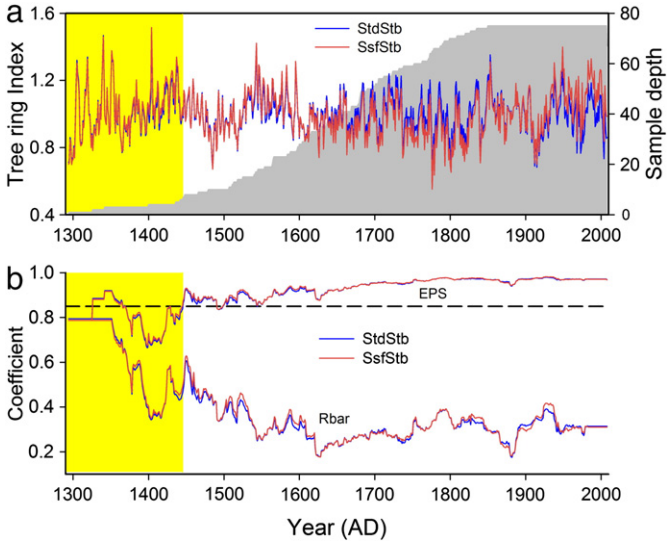


**Figure 2.** The chronology indices before (blue line) and after (red line) signal-free iterations and the sample depth (number of cores; gray shape) (a), as well as the running Rbar and the running expressed population signal (EPS) (based on a 51-yr window with 1-yr lag) (b). The shaded yellow box indicates the period from 1294 to 1445 when the sample depth is low and less confidence is placed in the chronology. The reliable portion of the chronology is defined as times with an EPS value greater than 0.85 (dashed black line).

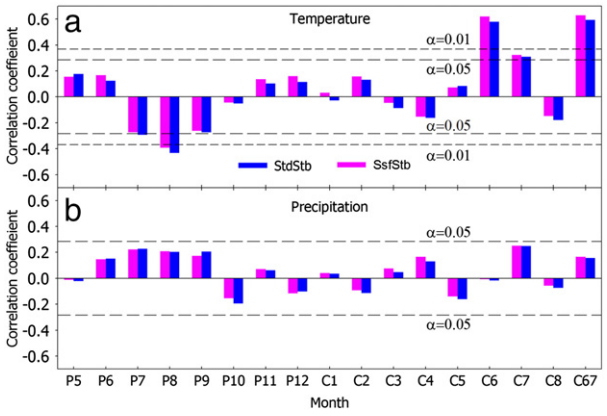


**Figure 3.** Correlation between tree-ring chronologies and time series of temperature (a) and precipitation (b). P and C mark the previous and current year, respectively. Numbers indicate months; for example, C6 indicates the current June and C67 means current June to July.

precipitation were not significant. The highest correlation ($r = 0.629$) was found between the SsfStb chronology and the regional mean June to July temperature.

Because temperatures in the boreal and temperate forests are currently below the trees' temperature optimum (Way and Oren, 2010) and the forests in the study area are at high elevation, warmer temperatures would increase the trees' growth rates. Correlation of tree growth with early-summer temperature has been found at many sites in the southeastern Tibet Plateau: e.g., Shao and Fan (1999) found that tree growth in the western Sichuan Plateau, a part of the southeastern Tibetan Plateau, was significantly related to the June mean temperature and the mean winter minimum temperature. In Maerkang, Yu et al. (2012) found that the tree-ring data most significantly correlated with the July temperature. Li et al. (2010, 2011) found that tree growth in the western Sichuan Plateau was dominated by June to August temperature in Wolong and by June to July temperature in Miyaluo. In Jiuzhaigou, Song et al. (2007) found that tree growth significantly correlated with the mean June temperature and the minimum temperature of the winter half year.

A significant negative correlation of tree growth with the late summer temperature of the previous year has not been noted in prior studies in the southeastern Tibet Plateau. This correlation with the previous year's temperatures may indicate the trees' ability to use the previous year's photosynthesis product for the next year's growth. Because regional precipitation peaks in June and temperature peaks in July (Fig. 1), the soil moisture condition should be wetter in June than in the following months. Therefore, the negative correlation with temperature probably occurs because of soil moisture conditions. This inference is supported by the positive, though not significant, correlation of tree growth with the precipitation of the previous July, August and September and the current July. This possible temperature-induced drought effect can also be observed in the current July, as the positive correlation between the tree growth and July temperature decreases and the positive correlation with July precipitation increases (although not significantly) compared to June, indicating that suitable temperature and soil moisture are very important factors for tree growth at this high-elevation site. In conclusion, low temperature in June to July is the major limiting factor for tree growth, and extremely high temperature in July may also limit tree growth.

Another important difference between our results and those of previous studies is the limited correlation ($r < 0.2$) with winter temperature. A possible explanation is the high elevation of our study site (~4300 m asl), which means it may be covered by insulating snow in winter, raising and stabilizing the soil temperature (Decker et al., 2003). Therefore, higher winter temperatures have a limited benefit to the trees in our study site. Previous studies (Shao and Fan, 1999; Song

https://doi.org/10.1016/j.yqres.2013.08.002 Published online by Cambridge University Press

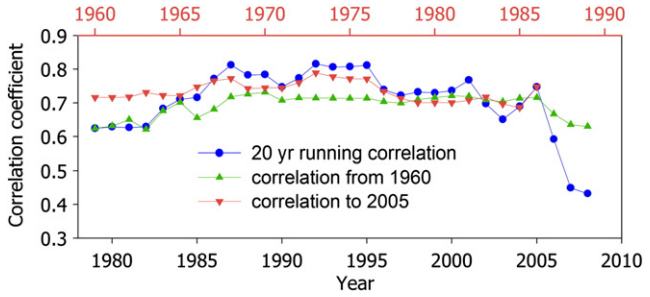


**Figure 4.** Correlation coefficients between the tree-ring chronology and June–July temperature. Circles (blue) show the 20-yr running correlations, with the values plotted at the end of the 20-yr windows (lower axis); triangles (green) show the correlations for periods from 1960 to the years on the lower axis; inverted triangles (red) show the correlations for periods from the years on the upper axis to 2005.

et al., 2007; Li et al., 2011; Yu et al., 2012) were at lower elevations (approximately 3000–3900 m asl) that may have less snow and would thus be more sensitive to winter temperature.

The running correlations between the SsfStb chronology and the best-correlated climate variable, the current June to July mean temperature, show that the correlation abruptly decreased in the last three years (Fig. 4). The unstable relationship with the climate variables, especially temperature, has also been noted in many other studies (e.g., D'Arrigo et al., 2008; Gao et al., 2013). Several mechanisms have been proposed to explain this phenomenon, including more stress from temperature-induced drought, exceeding the optimal growing temperature due to recent global warming, and decreases in the amount of solar radiation available for photosynthesis and plant growth ('global dimming'), among others (D'Arrigo et al., 2008). In this study, we found that 2006 was the warmest year in the past 49 yr. Because higher temperatures would increase moisture elimination, this consistent with the increase (decrease) of correlation between growth rates and precipitation (temperature) in July compared to June.

Correlation analysis with a fixed start year (1960) and a varying end year (ranging from 1979 to 2008) showed that an overall correlation decrease occurred over the last several years (Fig. 4). Correlation coefficients with a fixed end year (2005) and a varying start year (ranging from 1960 to 1976), though, varied little over the entire period. Therefore, we eliminated the last three years and used only the interval 1960–2005 for calibration and verification.

### *Calibration and verification of the reconstruction model*

We used the instrumental data from 1960 to 2005 to design a linear regression model to describe the relationship between tree-ring index (I) and regional mean temperature in June to July ($T_{67}$). The model is as follows:

$$T_{67} = 3.708 * I + 9.864.$$

The correlation coefficient of the function is 0.715 ($n = 46$, $p < 0.001$). The regression model accounts for 51.2% ($R^2_{adj} = 50.1\%$, $F = 46.15$) of the variance in instrumental temperature over the calibration period from 1960 to 2005 (Table 1). A split-period calibration verification scheme was applied. The statistics used were Pearson correlations, the sign tests of undifferenced data (ST) and first-differenced data (ST1), the reduction of error (RE) and the coefficient of efficiency (CE). As shown in Table 1, the statistics were all passed ($p < 0.05$ or positive RE/CE), indicating that the reconstruction was stable over the entire period (Cook and Kairiukstis, 1990). The reconstructed temperature variations were very consistent with the instrumental data at low frequency (Fig. 5a), but at high frequency, the reconstruction could not fully capture the magnitude of the extremely cold years (e.g., 1982, 1985 and 1990); this may be partly because in cold years, trees can use material and energy stored from the previous year.

### *June–July temperature variations*

Based on the linear regression model, we reconstructed regional June to July mean temperatures for the southeastern Tibet Plateau back to AD 1446 (Fig. 5b). The mean of the reconstructed temperature from 1446 to 2008 is 13.54 °C. Extremely warm years (at least two standard deviations above the mean, where one standard deviation is $\sigma = 0.49$°C) occurred in 1542, 1543, 1546, 1547, 1583, 1595, 1853, 1938, 1949, 1951, 1983, 1987 and 1999. Extremely cold years (at least $2\sigma$ below the mean) were found in 1485, 1776, 1777, 1779, 1793, 1798, 1800, 1801, 1819, 1840, 1912 and 1915. It appears that the extremely warm years were concentrated in the 16th and the 20th centuries. To highlight the multi-decadal temperature variations, the annual values were smoothed with a 20-yr low-pass filter (Fig. 5b). We defined a cold spell as a period with filtered temperature continuously below average for more than 10 yr, and a warm spell as an interval with filtered temperature continuously above average for more than 10 yr. Using these metrics, we identified seven cold periods and six warm periods in the reconstruction. Cold periods were from AD 1472 to 1524, 1599 to 1653, 1661 to 1715, 1732 to 1828, 1837 to 1847, 1865 to 1876 and 1907 to 1926. Warm intervals occurred from AD 1446 to 1471, 1525 to 1598, 1716 to 1731, 1848 to 1864, 1877 to 1906 and 1927 to present. The temperature was generally low from about 1600 to 1850, coinciding with the little ice age which has been documented from many regions of the globe.

Spatial field correlations between instrumental records and a gridded 0.5° × 0.5° June–July temperature dataset for a self-defined region (CRU TS 3.1; Mitchell and Jones, 2005) for the period 1960–2005 reveal significant ($p < 0.05$) temperature correlations across a large geographic region (Fig. 6a). Spatial correlations derived from our reconstructed temperature and the CRU gridded dataset show a similar general pattern, although the correlations are stronger for the instrumental records (Fig. 6b). This discrepancy could be due to the loss of variance in our reconstruction model. These results suggest that our reconstructions provide some information about the June–July temperature variability for the region around the southeastern Tibetan Plateau and the Yungui Plateau (Fig. 6).

To test the spatial representation of the reconstruction further, we compared our reconstructed temperature series with two other summer temperature series reconstructed from tree rings. These records are circumjacent to our study region and extend considerably far into the

**Table 1**
Statistics of the split calibration-verification model for the temperature reconstruction in the southeastern Tibet Plateau.

| Calibration | | | | | | Verification | | | | | |
|---|---|---|---|---|---|---|---|---|---|---|---|
| Period | r | $R^2$ | $R^2_{adj}$ | ST | ST1 | Period | r | ST | ST1 | RE | CE |
| 1960–1982 | 0.621 | 0.386 | 0.357 | 17/6 | 19/3 | 1983–2005 | 0.717 | 19/4 | 20/2 | 0.677 | 0.496 |
| 1983–2005 | 0.717 | 0.514 | 0.491 | 20/3 | 20/2 | 1960–1982 | 0.621 | 18/5 | 19/3 | 0.594 | 0.380 |
| 1960–2005 | 0.715 | 0.512 | 0.501 | | | | | | | | |

Symbols: r, Pearson correlation coefficient; $R^2$, explained variance; $R^2_{adj}$, explained variance after adjustment for the loss of degrees of freedom; ST, the sign test of the undifferenced data; ST1, the sign test of the first difference; RE, reduction of error; CE, coefficient of efficiency. All correlation coefficients and sign test values are statistically significant ($p < 0.05$).

https://doi.org/10.1016/j.yqres.2013.08.002 Published online by Cambridge University Press

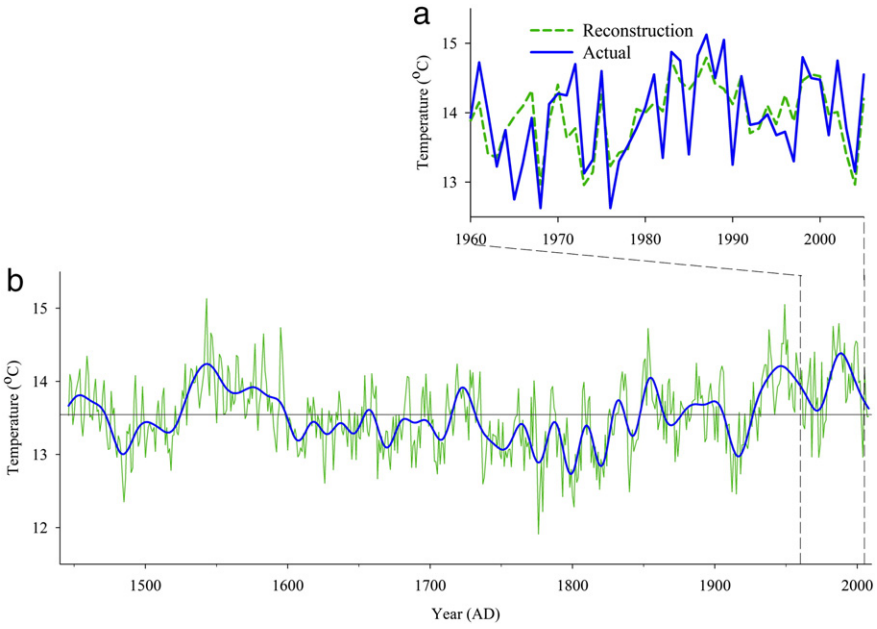


**Figure 5.** Comparison between the reconstructed and actual temperature during the calibration period 1960–2005 (a); the reconstructed June-July temperature using the reliable period of the SsfStb chronology from 1446 to 2008 (b). The thick line in (b) indicates the 20-yr low-pass filtered time series.

past (Fig. 7). The results show that our temperature series corresponds closely with the reconstructed summer minimum temperature in the source region of the Yangtze River (Liang et al., 2008) (Fig. 7a) and with the reconstructed August temperature of the southeastern Tibetan Plateau (Zhu et al., 2011) (Fig. 7b). The records share common cool periods from 1905 to 1925 and 1965 to 1980, comparable warm periods from 1925 to 1965 and 1980 to present and similar temperature fluctuations from 1765 to 1890. Our series also agrees well with the reconstruction by Zhu et al. (2011) from 1590 to 1660 and from 1680 to 1750 (Fig. 7b) and exhibits a significant cool period from 1660 to 1680 that also appears in the reconstruction by Liang et al. (2008).

Our reconstruction also agrees well with other reconstructions in the larger region. For example, our series is similar to the reconstructed July temperature at Maerkang in the early 18th century, the 19th century and the middle 20th century (Yu et al., 2012). The peaks and troughs of our reconstruction from 1700s to 1950s correspond closely with warm and cold periods of the reconstructed summer temperature variations in the central Hengduan Mountains (Li et al., 2012). Our series is also similar to tree-ring-recorded temperature variations in May through August in the Gaoligong Mountains (Fan et al., 2010) in the 17th century. The warm temperatures in the 16th century and the warming of the last two centuries seen in our record also appear in the reconstructed Northern Hemisphere temperature series (D'Arrigo et al., 2006) (Fig. 7d).

The above analysis shows that our reconstruction agrees well with other summer temperature reconstructions in the study area, in nearby regions of the continent, and in the Northern Hemisphere in general. This suggests that our reconstruction has good spatial representation.

### *Possible forcing mechanism*

MTM analysis reveals significant (95% confidence level) cycle peaks at 2.0, 2.2–2.4, 2.7, 3.0–3.3, 3.7, 5.6–6.0, 10.7, 51.2, 102.2 and 204.8 yr (Fig. 8). The 2–6 yr signals correspond to the El Niño Southern Oscillation timescale (Philander, 1983). Low-frequency temperature variations in the southeastern Tibet Plateau also show a clear resemblance

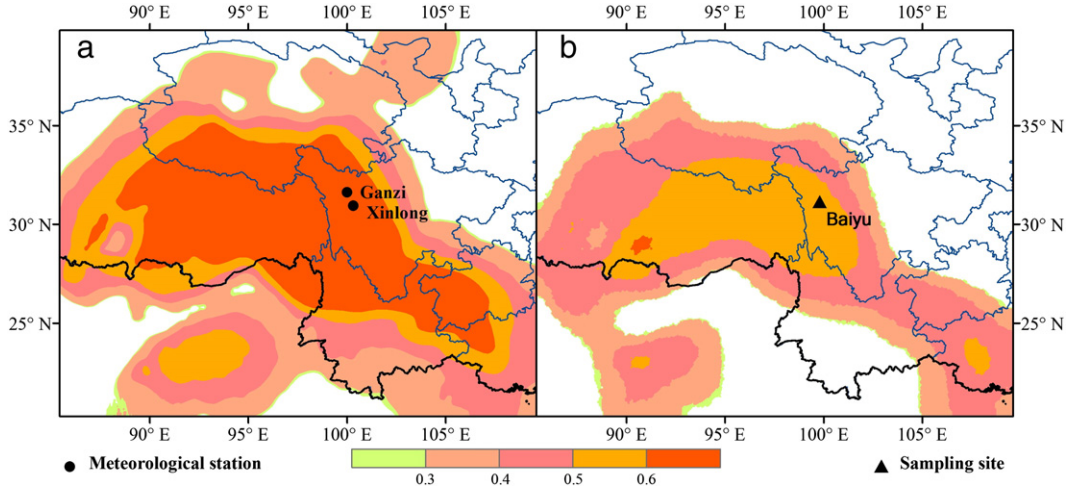


**Figure 6.** Spatial correlation of June–July temperature for the southeastern Tibet Plateau from the concurrent CRU TS3.1 0.5° × 0.5° grid (Mitchell and Jones, 2005) with the regional instrumental record (a) and our tree-ring reconstructed record (b). Temperature data are over the period AD 1960–2005. Only significant ($p < 0.05$) correlations are shown.

https://doi.org/10.1016/j.yqres.2013.08.002 Published online by Cambridge University Press

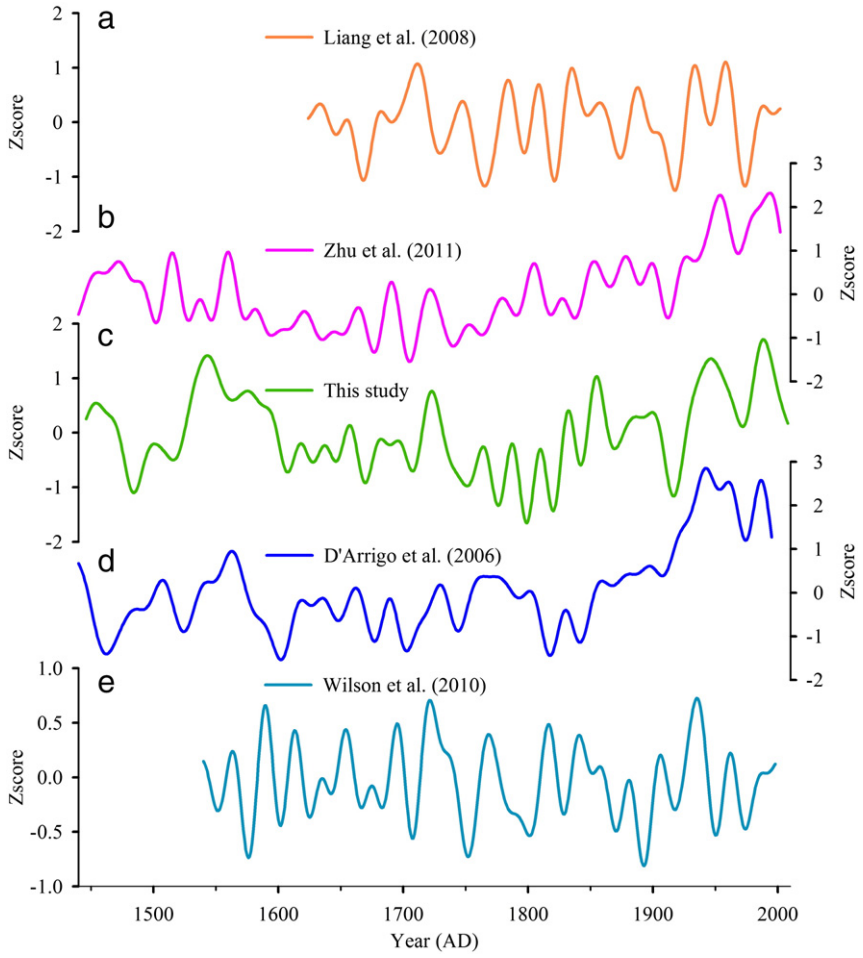


**Figure 7.** Comparisons between the reconstructed summer minimum temperature in the source region of the Yangtze River (Liang et al., 2008) (a), the reconstructed August temperature of southeastern Tibetan Plateau (Zhu et al., 2011) (b), our reconstructed regional June–July temperature (c), the reconstructed North Hemisphere temperature (D'Arrigo et al., 2006) (d) and the ENSO reconstruction (Wilson et al., 2010) (e). The time series were all smoothed with a 20-yr low-pass filter.

to the reconstructed ENSO series (Wilson et al., 2010) (Fig. 7e), indicating that ENSO may affect the temperature of the study area. During a warm phase of ENSO, the strength of the Indian monsoon is reduced due to the subsidence of the tropical Walker circulation extending from the western Pacific to the Indian subcontinent (Kumar et al., 1999). A weaker Indian monsoon will decrease precipitation, thus reducing the cooling effect of precipitation and subsequent evaporation on the regional surface air temperature (Ding and Chan, 2005), which results in above-normal temperatures. Similarly, the cool phase of ENSO should result in cooler-than-normal temperatures in our study area. Nearby studies also found a negative correlation between the ENSO index and regional drought severity (Fang et al., 2010).

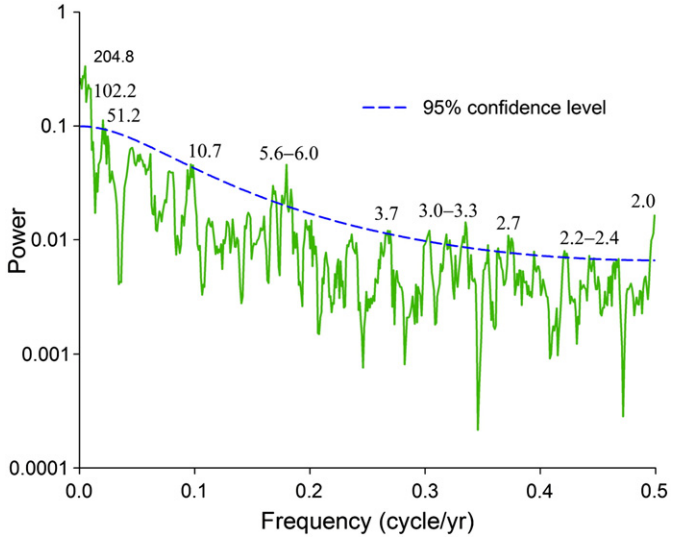


**Figure 8.** Multi-taper method (Mann and Lees, 1996) power spectrum of the reconstructed June to July temperature for the period AD 1446–2008. The 95% confidence level relative to red noise is shown by the dashed curve. The numbers refer to the significant peaks in yr.

The decadal variability peaks found at 10.7 yr and 51.2 yr may correspond to the Schwabe cycle of solar activity (Braun et al., 2005) and Pacific Decadal Oscillation (PDO) (Minobe, 1997) time scales, respectively, whereas the centennial cycles at 102.2 yr and 204.8 yr may be related to the Gleissberg and the Suess solar cycles (Braun et al., 2005), respectively. There has been evidence of the solar effect on climate change at many nearby sites (e.g., Wang and Zhang, 2011).

## Conclusions

We have developed a 715-yr tree-ring-width chronology using the signal-free method, which we have applied to reconstruct the June–July temperature for the southeastern Tibet Plateau over the past 563 yr. This reconstruction explains 51.2% of the variance of the instrumental temperature record over the period from 1960 to 2005. Spatial correlation analyses suggest that the temperature reconstruction is the representative of the southeastern Tibetan Plateau, the Yungui Plateau and their vicinity. The reconstructed temperature series corresponds

https://doi.org/10.1016/j.yqres.2013.08.002 Published online by Cambridge University Press

well with other tree-ring-based temperature reconstructions on the decadal scale, further indicating that the reconstructed temperature series may also reflect regional temperature variability. Spectral analyses and the comparison of time series both suggest that the temperature variability in this area may be affected by ENSO, the PDO and solar activity.

## Acknowledgments

This is a paper in celebration of Professor Jijun Li's 80th birthday and his academic career, theories and achievements. The authors thank Prof. Eryuan Liang and Dr. Haifeng Zhu who kindly provided their reconstruction data for comparison and Professor Ed Cook for a 'signal-free' version of ARSTAN. The authors also thank senior editor Professor Alan Gillespie, guest editor Professor Fahu Chen and two reviewers for their valuable comments and suggestions. This research was supported by the National Science Foundation of China (No. 41171039 and No. 41021091), the Program of Introducing Talents of Discipline to Universities from China's Ministry of Education (No. B06026) and the Doctoral Fund of Ministry of Education of China (20120211110041).

## References

Braun, H., Christl, M., Rahmstorf, S., Ganopolski, A., Mangini, A., Kubatzki, C., Roth, K., Kromer, B., 2005. Possible solar origin of the 1,470-year glacial climate cycle demonstrated in a coupled model. Nature 438, 208–211.

Cohen, J.L., Furtado, J.C., Barlow, M., Alexeev, V.A., Cherry, J.E., 2012. Asymmetric seasonal temperature trends. Geophysical Research Letters 39, L04705.

Cook, E.R., Kairiukstis, L.A., 1990. Methods of Dendrochronology. Kluwer Dordrecht.

D'Arrigo, R., Wilson, R., Jacoby, G., 2006. On the long-term context for late twentieth century warming. Journal of Geophysical Research D: Atmospheres 111, D03103.

D'Arrigo, R., Wilson, R., Liepert, B., Cherubini, P., 2008. On the 'Divergence Problem' in Northern Forests: a review of the tree-ring evidence and possible causes. Global and Planetary Change 60, 289–305.

Decker, K.L.M., Wang, D., Waite, C., Scherbatskoy, T., 2003. Snow removal and ambient air temperature effects on forest soil temperatures in northern Vermont. Soil Science Society of America Journal 67, 1234–1242.

Ding, Y., Chan, J.C.L., 2005. The East Asian summer monsoon: an overview. Meteorology and Atmospheric Physics 89, 117–142.

Domrös, M., Peng, G., 1988. The Climate of China. Springer-Verlag.

Duan, J., Wang, L., Li, L., Chen, K., 2010. Temperature variability since A.D. 1837 inferred from tree-ring maximum density of *Abies fabri* on Gongga Mountain, China. Chinese Science Bulletin 55, 3015–3022.

Fan, Z., Bräuning, A., Tian, Q., Yang, B., Cao, K., 2010. Tree ring recorded May–August temperature variations since A.D. 1585 in the Gaoligong Mountains, southeastern Tibetan Plateau. Palaeogeography, Palaeoclimatology, Palaeoecology 296, 94–102.

Fang, K.Y., Gou, X.H., Chen, F.H., Li, J.B., D'Arrigo, R., Cook, E., Yang, T., Davi, N., 2010. Reconstructed droughts for the southeastern Tibetan Plateau over the past 568 years and its linkages to the Pacific and Atlantic Ocean climate variability. Climate Dynamics 35, 577–585.

Gao, L., Gou, X., Deng, Y., Liu, W., Yang, M., Zhao, Z., 2013. Climate–growth analysis of Qilian juniper across an altitudinal gradient in the central Qilian Mountains, northwest China. Trees - Structure and Function 27, 379–388.

Gou, X., Chen, F., Yang, M., Gordon, J., Fang, K., Tian, Q., Zhang, Y., 2008. Asymmetric variability between maximum and minimum temperatures in Northeastern Tibetan Plateau: evidence from tree rings. Science in China Series D: Earth Sciences 51, 41–55.

Holmes, R.L., 1983. Computer-assisted quality control in tree-ring dating and measurement. Tree-Ring Bulletin 43, 69–78.

IPCC, 2007. Climate Change 2007: The Physical Science Basis: Contribution of Working Group I to the Fourth Assessment Report of the Intergovernmental Panel on Climate Change. Cambridge University Press.

Kamenos, N.A., 2010. North Atlantic summers have warmed more than winters since 1353, and the response of marine zooplankton. Proceedings of the National Academy of Sciences 107, 22442–22447.

Kumar, K.K., Rajagopalan, B., Cane, M.A., 1999. On the weakening relationship between the Indian monsoon and ENSO. Science 284, 2156–2159.

Li, Z., Liu, G., Zhang, Q., Hu, C., Luo, S., Liu, X., He, F., 2010. Tree ring reconstruction of summer temperature variations over the past 159 years in Wolong National Natural Reserve, western Sichuan, China. Chinese Journal of Plant Ecology 34, 628–641 (In Chinese with English Abstract).

Li, Z., Liu, G., Fu, B., Zhang, Q., Hu, C., Luo, S., 2011. Tree-ring based summer temperature reconstruction over the past 200 years in Miyaluo of western Sichuan, China. Quaternary Sciences 31, 522–534 (In Chinese with English Abstract).

Li, Z., Zhang, Q., Ma, K., 2012. Tree-ring reconstruction of summer temperature for A.D. 1475–2003 in the central Hengduan Mountains, Northwestern Yunnan, China. Climatic Change 110, 455–467.

Liang, E.Y., Shao, X.M., Qin, N.S., 2008. Tree-ring based summer temperature reconstruction for the source region of the Yangtze River on the Tibetan Plateau. Global and Planetary Change 61, 313–320.

Mann, M.E., Lees, J.M., 1996. Robust estimation of background noise and signal detection in climatic time series. Climatic Change 33, 409–445.

Melvin, T.M., Briffa, K.R., 2008. A "signal-free" approach to dendroclimatic standardisation. Dendrochronologia 26, 71–86.

Minobe, S., 1997. A 50–70 year climatic oscillation over the North Pacific and North America. Geophysical Research Letters 24, 683–686.

Mitchell, T.D., Jones, P.D., 2005. An improved method of constructing a database of monthly climate observations and associated high-resolution grids. International Journal of Climatology 25, 693–712.

Philander, S., 1983. El Niño southern oscillation phenomena. Nature 302, 295–301.

Shao, X., Fan, J., 1999. Past climate on west Sichuan plateau as reconstructed from ring-widths of dragon spruce. Quaternary Sciences 81–89 (In Chinese with English Abstract).

Song, H., Liu, Y., Ni, W., Cai, Q., Sun, J., Ge, W., Xiao, W., 2007. Winter mean lowest temperature derived from tree-ring width in Jiuzhaigou region, China since 1750 A.D. Quaternary Science 27, 486–491 (In Chinese with English Abstract).

Wang, X., Zhang, Q., 2011. Evidence of solar signals in tree rings of Smith fir from Sygera Mountain in southeast Tibet. Journal of Atmospheric and Solar-Terrestrial Physics 73, 1959–1966.

Way, D.A., Oren, R., 2010. Differential responses to changes in growth temperature between trees from different functional groups and biomes: a review and synthesis of data. Tree Physiology 30, 669–688.

Wigley, T., Briffa, K.R., Jones, P.D., 1984. On the average value of correlated time series, with applications in dendroclimatology and hydrometeorology. Journal of Applied Meteorology 23, 201–213.

Wilson, R., Cook, E., D'Arrigo, R., Riedwyl, N., Evans, M.N., Tudhope, A., Allan, R., 2010. Reconstructing ENSO: the influence of method, proxy data, climate forcing and teleconnections. Journal of Quaternary Science 25, 62–78.

Wu, P., Wang, L., Shao, X., 2005. Reconstruction of summer temperature from maximum latewood density of *Pinus densata* in West Sichuan. Acta Geographica Sinica 60, 998–1006 (In Chinese with English Abstract).

Xu, H., Hong, Y.T., Hong, B., Zhu, Y.X., Wang, Y., 2010. Influence of ENSO on multi-annual temperature variations at Hongyuan, NE Qinghai–Tibet plateau: evidence from $\delta^{13}C$ of spruce tree rings. International Journal of Climatology 30, 120–126.

Yu, S., Yuan, Y., Wei, W., Zhang, T., Shang, H., Chen, F., 2012. Reconstructed mean temperature in Mearkang, West Sichuan in July and its detection of climatic period signal. Plateau Meteorology 31, 193–200 (In Chinese with English Abstract).

Zhu, H., Shao, X., Yin, Z., Xu, P., Xu, Y., Tian, H., 2011. August temperature variability in the southeastern Tibetan Plateau since AD 1385 inferred from tree rings. Palaeogeography, Palaeoclimatology, Palaeoecology 305, 84–92.

https://doi.org/10.1016/j.yqres.2013.08.002 Published online by Cambridge University Press